DOI: 10.19884/j.1672-5220.202405013

Fault Detection of Yarn Congestion in Sizing Machine Based on Machine Vision

LI Jingwei, ZOU Kun*, ZHAO Chen
College of Mechanical Engineering, Donghua University, Shanghai 201620, China

Abstract: During the sizing process, yarn congestion fault occurs at the reed teeth of a sizing machine. At present, the yarn congestion fault is generally handled by manual detection. The sizing production line operates on a large scale and runs continuously. Untimely handling of the yarn congestion fault causes a large amount of yarn waste. In this research, a machine vision-based algorithm for yarn congestion fault detection is developed. Through the analysis of the congestion fault and interference contour characteristics, the basic idea of image phase subtraction to identify the congestion fault is determined. To address the interference information appearing after image phase subtraction, the image pre-processing methods of Canny edge extraction and mean filtering are employed. According to the fault size and location characteristics, the fault contour detection algorithm based on inter-frame difference is designed. To mitigate the camera vibration interference, the anti-vibration interference algorithm based on affine transformation is studied, and the fault detection algorithm for the total yarn congestion fault is determined. The detection of 20 sets of field data is carried out, and the detection rate reaches 90%. This fault detection algorithm realizes the automatic detection of yarn congestion fault of sizing machine with certain real-time performance and accuracy.

Keywords: machine vision; yarn congestion; fault detection; inter-frame difference; affine transformation
CLC number: TP391.4 **Document code**: A
Article ID: 1672-5220(2025)03-0292-09

Open Science Identity (OSID)

0 Introduction

Sizing is an important process before weaving[1]. To improve the weavability of the yarn, it is necessary to ensure that the sizing process is carried out correctly[2]. At present, most of the spinning enterprises are using manual detection. Workers detect the sizing production line about 50 m long and deal with any faults on time. The environment of the workshop is harsh, with a lot of debris and dust, and the distance of the production line is long. Most of the sizing machines work 24 h a day, and when a fault occurs in the middle of the night, the workers are often unable to deal with it in time. Failure to detect the fault in time causes the accumulation of yarn in the faulty area, resulting in material waste and increased production costs. At the same time, the quality of the sizing yarn cannot be guaranteed, which affects the economic efficiency of the enterprise.

Machine vision is a branch of artificial intelligence. It is a computer simulation of human vision to judge and detect objective things. Through the image ingestion equipment, the object can be converted into an image and sent to the image processing system[3]. The image processing system converts the image into digital signals according to its pixels, colors and textures. It then processes the digital signals to obtain the target features, and sends commands to the machine based on the results of comparing the target features with the set parameters[4]. Machine vision is widely used in the textile industry for yarn detection[5-7]. Haleem et al.[8] implemented an online yarn detection system that combined image acquisition with the Viola-Jones target detection algorithm, achieving a success rate of 92% in detecting yarn knot defects. However, the test results of this system are different from those tested with a yarn uniformity tester, and the field feasibility is unknown. Xu et al.[9] proposed a yarn contour detection method based on knowledge-enhanced deep learning. The quality detection error can be reduced from about 1.5% to a tolerable 0.5%. However, a universal contour detection model for more types of yarns and other industrial applications needs to be developed. Dlamini et al.[10] utilized data preprocessing techniques to decompose the image into small pieces, adopted mean filtering to smooth the noise and applied affine transformation for data enhancement to diversify the data. They also used Gaussian filtering to enhance the information of hidden defects. Zuo et al.[11] used the Fourier transform to reconstruct images based on a machine vision system to detect knife-edge defects on the surface of magnetic sheets. Khanal et al.[12] utilized convolutional neural networks in a deep learning architecture to detect hairiness defects in hairy textiles, and the average classification accuracy was 96%. However, this study was carried out in a laboratory, and more experimental verification was

Received date: 2024-05-21
Foundation item: National Key Research and Development Program of China (No. 2017YFB1304001)
* Correspondence should be addressed to ZOU Kun, email: kouz@dhu.edu.cn
Citation: LI J W, ZOU K, ZHAO C. Fault detection of yarn congestion in sizing machine based on machine vision. *Journal of Donghua University (English Edition)*, 2025, 42(3): 292-300.

needed in the face of more complex industrial environments. Gültekin et al.[13] presented a machine vision system for automatic detection of yarn bobbins and fabric defects, which was suitable for replacing manual detection. Musa[14] designed a yarn break detection device that consisted of a charge-coupled device (CCD) camera, a screen and a line laser emitter. The success rate of the experiment was high, and the feasibility of installing the device on a loom could be studied in the future. Xia et al.[15] built an image acquisition system and designed a real-time automatic detection system for wrap reed collision of the sizing machine based on machine vision. The system had high detection accuracy and real-time performance. However, the detection range was relatively narrow, focusing only on a limited area of the yarn. Additionally, no experiments or tests have been carried out in the production line conditions. Li et al.[16] enhanced the detection algorithm for surface defects in nonwoven materials by integrating machine vision and deep learning techniques. The improved algorithm demonstrated a satisfactory level of accuracy and speed. Given these advantages, it is worth considering for implementation in industrial production.

Although these studies demonstrate relatively high real-time performance and accuracy, most are laboratory-based and lack experimental verification in complex industrial conditions. Thus, their practical applicability remains uncertain. Based on machine vision, this research analyzes the characteristics of the yarn congestion fault at the reed teeth of the sizing machine in industrial conditions. The detection algorithm of reed teeth yarn support is studied to realize the automatic detection of yarn congestion fault of the sizing machine. In addition, the actual effect of the field is statistically analyzed, which provides a good practical application value.

1 Camera of Yarn Congestion Fault Detection

The yarn is sized on the sizing machine and the structure diagram of the sizing machine is shown in Fig. 1. The yarn is first unwound from the warp beam frame, through the tension adjustment device, and fed into the pulp tank area for sizing. Then it moves through the sub-stranding rollers for sub-stranding and dried by the drying device. Next, it is waxed by the waxing equipment, and the yarn after waxing is separated in the dry sub-stranding area. Finally, it is wound into a weaving bobbin at the head of the sizing machine[17].

The camera of yarn congestion fault detection is mounted above the head of the sizing machine by utilizing a gantry, as shown in Fig. 2.

During normal production line operation, when a yarn congestion fault is detected, the system alerts on-site workers for immediate response. The industrial control computer transmits the fault signal to a relay, triggering an alarm. For fault data collection and detection analysis, a camera-connected video recorder is provided.

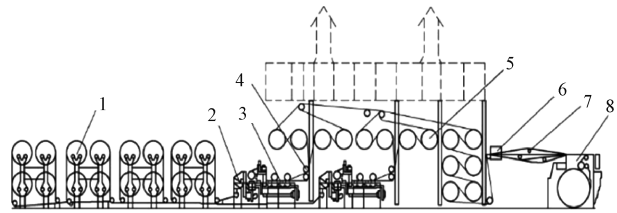

1—warp beam frame; 2—tension adjustment device; 3—pulp tank area; 4—sub-stranding rollers; 5—drying device; 6—waxing equipment; 7—dry sub-stranding area; 8—head of sizing machine.

Fig. 1 Structure diagram of sizing machine

Fig. 2 Camera mounting position

2 Basic Plan of Yarn Congestion Fault Detection

The sized yarn is carded by the reed teeth and eventually wound into a weaving bobbin for subsequent yarn weaving. Each yarn passes through a gap in the reed. If the reed teeth are unevenly carded, it may cause yarns to intertwine, or if the sizing effect is poor, it may lead to the adhesion of hairs from neighboring yarns. Both situations can result in yarn congestion fault at the reed teeth. Over time, this congestion can cause a build-up of yarn, ultimately leading to yarn wastage. Therefore, yarn congestion fault occurs on the side where the yarn enters the reed (Fig. 3).

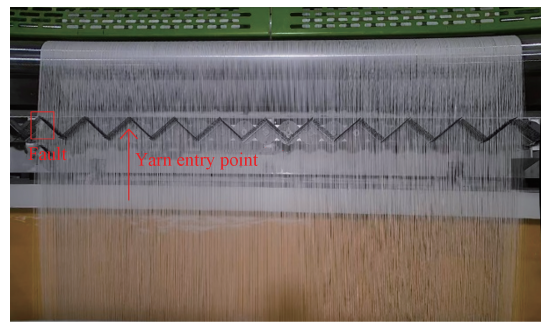

Fig. 3 Location of yarn congestion fault at reed teeth

At the beginning of the yarn congestion fault, the shape and size of the fault are not obvious. The fault sticks to the edge of the reed teeth and is located in human visual blind spots, making it difficult to detect. Over time, the oval-shaped yarn defect expands and entraps surrounding fibers, forming a dense cluster. Compared to normally aligned yarns, the fault region appears whiter, exhibits higher density, and displays well-defined edges, making it easily identifiable.

From the above fault characteristics, the basic plan of yarn congestion fault detection can be derived. Firstly, since the fault does not extend beyond the upper edge of the reed teeth, the detection area can be significantly reduced. Figures 4-6 illustrate a specific instance of a yarn congestion fault. The specific location of the fault is marked with a red box, as shown in Fig. 4. The region of interest (ROI) for fault detection is a rectangle, with its left and right boundaries fully containing the yarn boundary. Its upper boundary intersects at the upper apex of the reed teeth, and its lower boundary has a margin to fully contain large yarn mass faults. Secondly, when the fault initially occurs, the detection algorithm is not designed to detect it due to the difficulty of extraction and its minimal impact on line operation. Finally, as the fault progresses, the yarn congestion gradually expands. Image subtraction between normal and fault conditions reveals residual contours with defined geometric properties (height, width and area) within the ROI (Fig. 5). These characteristic contours serve as definitive indicators of yarn congestion fault.

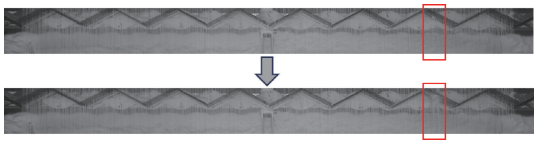

Fig. 4 Shape of yarn congestion fault changes over time

Fig. 5 Fault contours after image subtraction

During sizing line operation at speeds up to 100 m/min, machine-induced vibrations propagate through the gantry base, causing camera resonance. This vibration artifact manifests as reed teeth contours in differential image processing (normal image vs. vibration-affected image), creating primary interference for yarn congestion fault detection. The normal image is subtracted from the image containing vibration interference information and the result after extracting the ROI is shown in Fig. 6.

Fig. 6 Reed teeth contours after image subtraction

3 Algorithm for Yarn Congestion Fault Detection

The overall workflow of the yarn congestion fault detection algorithm is shown in Fig. 7. It involves the algorithms for image preprocessing, fault contour extraction, and anti-vibration interference. Through the software system to capture the real-time yarn images at the reed teeth position, each image is first judged whether it contains interference contours. When 10 images are captured, fault detection is performed on this group of images. If it is determined that a yarn congestion fault has occurred, the relevant identification bit triggers an alarm from the sizing vision software system and temporarily stops the yarn congestion fault detection. When the alarm is over, the capturing will be restarted. If it is determined that it is not a fault, the next image will be captured and the first captured image in the capture folder will be deleted.

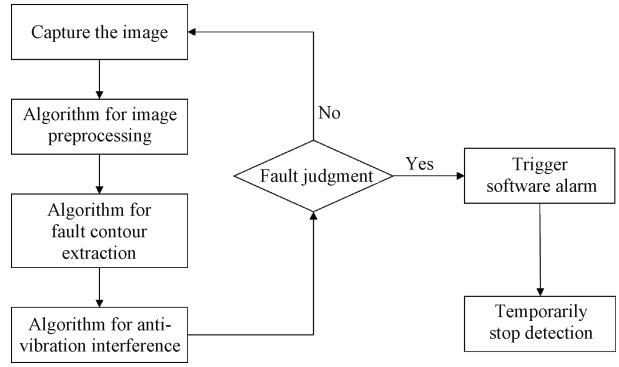

Fig. 7 Overall workflow of yarn congestion fault detection algorithm

3.1 Algorithm for image preprocessing

Image preprocessing performs noise reduction, rotation and enhancement to minimize irrelevant information interference, thereby improving accuracy in subsequent detection and edge extraction. The main preprocessing algorithms involved in yarn congestion fault detection are edge extraction and image filtering.

Yarn congestion fault detection requires edge extraction of the subtraction images. After extraction, the presence of a fault is determined by analyzing the shape and size features of the contours. In this research, the image was processed by Halcon software. An image with yarn congestion fault was selected and subtracted from the normal image, and three commonly used edge extraction algorithms, Sobel, Laplace and Canny, were used for the subtraction image. The extraction results are compared after binarization, as shown in Fig. 8.

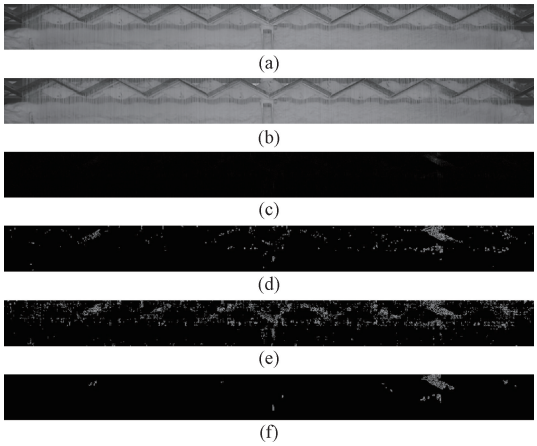

Fig. 8 Effects of different edge extraction operators: (a) normal image; (b) fault image; (c) original phase subtraction image; (d) Sobel operated image; (e) Laplace operated image; (f) Canny operated image

As can be seen from the fault image, the fault has occurred for a while and has a certain size. The fault is shown as a white spot in the original phase subtraction image, and no other interference points or contours are seen. From the processing results, the Sobel operator can extract the fault information very well, but it also detects a lot of independent noise points and burrs, and the size of the contours formed in the area where some of the noise points are concentrated may satisfy the fault detection threshold condition and may be misclassified as a fault. The extraction effect of the Laplace operator is poor, and the number of noise points is significantly increased compared with that of the Sobel operator, while the lower edge of the fault contour is fuzzy. This operator is greatly affected by the noise points and responds more strongly to isolated noise points than to edge lines. The double threshold judgment of the Canny operator greatly reduces the interference information, while the fault contours are more adequately extracted. In summary, the Canny operator is most suitable as an edge extraction operator for fault detection.

However, as can be seen from the processing effect of the Canny operator, it is difficult to entirely avoid the introduction of noise points and interference contours while extracting the fault. Therefore, it is necessary to introduce a filtering treatment before edge extraction. Three commonly used filtering methods, namely median filtering, mean filtering and Gaussian filtering, are compared and tested.

Before subtraction, the two images (Figs. 8(a) and 8(b)) were preprocessed using three filtering methods. The resultant images were then subtracted to enhance defect visibility. The effects of different filtering treatments are shown in Fig. 9.

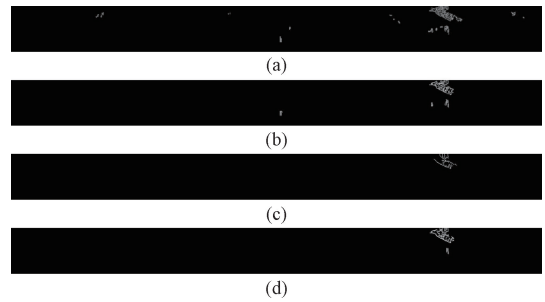

Fig. 9 Effects of different filtering treatments: (a) unfiltering; (b) median filtering; (c) mean filtering; (d) Gaussian filtering

It can be seen that the mean filtering method removes the most interference contours and retains enough fault information, and the height, width and area features of the fault contours still meet the threshold conditions of fault features. In summary, mean filtering is selected as the image-filtering method for fault detection.

3.2 Algorithm for fault contour extraction

The image is preprocessed to extract a variety of contours, and the size characteristics of the contours are analyzed to determine whether they are fault contours. If the fault is judged by subtracting only two images, although the judgment speed is fast, the false alarm rate is high. Therefore, multiple images should be set to subtract, and the contours of multiple subtraction images within a period will meet the threshold conditions before they are recognized as faults, to improve the detection accuracy.

The inter-frame difference is a method of subtracting two images in a video stream that are separated by several frames. With this method, it is possible to detect the region that has changed in the two images. Yarn congestion fault is the cause of change and is suitable for detection using the inter-frame difference method. Since the fault may remain unchanged after a while of getting bigger, most of the fault information will be lost by using the subtraction of two adjacent frames. Therefore, the first image is selected as the standard image, and the method of subtracting the first image from the next nine images is used. The time of yarn congestion fault detected by this algorithm is mainly affected by the time interval between two adjacent frames of images taken by the inter-frame difference method. After field experiments, if the detection time of the yarn congestion fault detection algorithm is too short, the accuracy will be low. If the detection time is too long, the real-time performance will be insufficient. After the trade-off comparison, the time interval between the images taken by the inter-frame difference method is set to 6 s, and the time for the algorithm to detect yarn congestion fault is controlled at about 60 s. At this time, the real-time performance and accuracy can meet the production needs.

To quantify the dynamic changes in yarn images, the inter-frame difference $d_k(u,v)$ is calculated by

$$d_k(u,v) = f_k(u,v) - f_1(u,v), \quad (1)$$

where $f_k(u,v)$ is the current frame; $f_1(u,v)$ is the first frame; u and v represent abscissa and ordinate position information of the pixel, respectively. A set of faulty images is shown in Fig. 10.

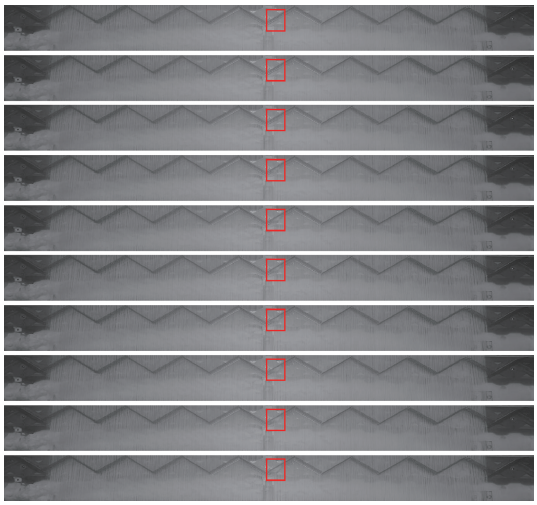

Fig. 10 Sequential multi-frame images of yarn congestion fault

The fault initially appeared in the fourth image and gradually expanded thereafter. We applied mean filtering to a sequence of nine images, subtracted the first image from the filtering result, and then performed edge extraction. Contours were screened based on their height, width and area, with the final results shown in Fig. 11.

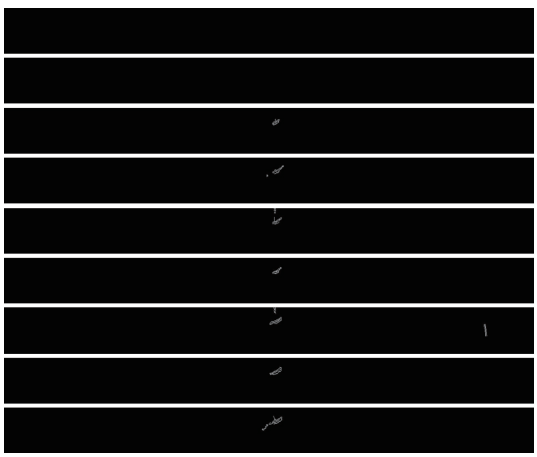

Fig. 11 Images of extracting contours after image subtraction

It can be seen that the vertically oriented interference contours still exist above the fault contours in the fifth and seventh images, and the diagonally oriented interference contours exist on the right side of the seventh image. In addition to the size characteristics, the fault contours are also characterized by little change in the horizontal coordinate position over time, while the position of the interference contours is random and is not affected by the position of the yarn congestion fault. Through multiple sets of fault image testing, the threshold conditions for identifying congestion fault contours are established as follows: contour height larger than eight pixels, width larger than seven pixels and area larger than 20 pixels. Furthermore, a fault is confirmed when contours appear at three or more similar horizontal positions (positional offset within 10 pixels) in nine phase-subtraction images. The detailed workflow of the yarn congestion fault detection algorithm based on contour thresholds is shown in Fig. 12.

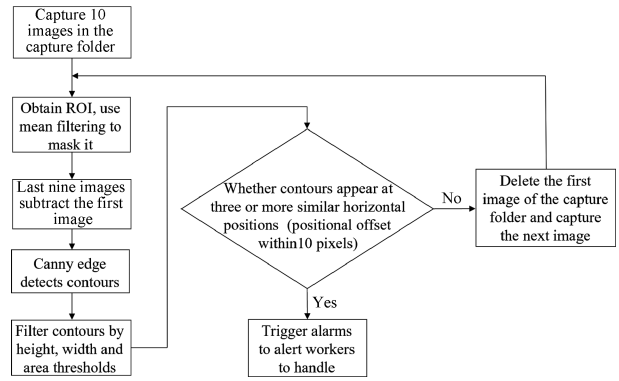

Fig. 12 Detailed workflow of yarn congestion fault detection algorithm based on contour thresholds

3.3 Algorithm for anti-vibration interference

Under high-speed operating conditions of the sizing machine, excessive yarn speed occasionally occurs, inducing machine vibration. The vibration propagates to both the gantry structure and the camera assembly. During image subtraction under vibration, due to the misalignment between the two images, the reed teeth contours are reduced. Subsequent images are affected by vibration interference, and subtracting the first image produces similar contours, as shown in Fig. 13.

Fig. 13 Nine subtraction images with reed teeth contours

The diagonal contours obtained by phase subtraction are caused by the misalignment of the W-shaped reed teeth between the two images. The diagonal contours of the reed teeth are long and thin, while the fault is in the

shape of a mass. The diagonal contours are close to or larger than the fault contours from the aspect ratio, which meets all the requirements of the fault detection algorithm for determining the contours as a fault and will cause a false alarm. Due to the misalignment between the images, a small amount of vertical and point-like contours of the yarn will still be subtracted with the filtering algorithm in place. If only oblique contours can be eliminated, the remaining vertical and point-like contours can be filtered out by length and width thresholds.

The interference contours are caused by the vibration-induced misalignment of the to-be-detected area between the images. If the first image is used as a reference image, and the positions of the next nine images are adjusted by panning and rotating so that their to-be-detected areas are aligned with the first image, the interference due to the misalignment between the images can be eliminated. Since the W-shaped reed teeth have clear contours, they are suitable for detection by using shape template matching.

Shape template matching was performed by using Halcon software. The shape feature information of the W-shaped reed teeth region is extracted in the first image to create a shape template, as shown in Fig. 14. The created shape template records the shape feature information such as contours, corner points and spots of the target shape, and it is used to subsequently find similar shapes in other images for matching.

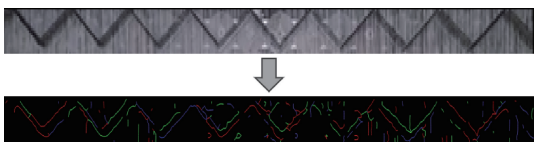

Fig. 14 Creation of a shape template

The next step is to find the region in the new input image that is most similar to the pre-defined shape template. The basic principle is to compare the shape templates at different positions in the new input image, find the most matching position, and return the matching result, including position and rotation angle information, which can be used for subsequent localization. The position information indicates the center position of the shape template found in the input image, which is represented by the pixel coordinate (x, y), where x is the abscissa of the center position and y is the ordinate of the center position. The rotation angle information represents the rotation angle of the shape template in the input image, expressed in radians.

By matching the shape template on the first image, the center position coordinate (x_0, y_0) of the W-shaped reed teeth region is obtained. The ith of the next nine images are matched to get the center position coordinate (x_i, y_i) and the rotation angle α_i. The horizontal coordinate offset of the W-shaped reed teeth area in the ith of the next nine images is $x_{\Delta i} = x_i - x_0$, the vertical coordinate offset is $y_{\Delta i} = y_i - y_0$, and the rotation angle offset is $\alpha_{\Delta i} = \alpha_i - \alpha_0$.

$\boldsymbol{E}$ is the identity matrix; $\boldsymbol{A}$ is the radial transformation matrix after adding translation transformation; $\boldsymbol{B}$ is the affine transformation matrix after adding rotation transformation. The affine transformation of translation and rotation can be performed on the next nine images to align their area to be detected with the first image.

Define an identity matrix

$$\boldsymbol{E} = \begin{bmatrix} 1 & 0 & 0 \\ 0 & 1 & 0 \\ 0 & 0 & 1 \end{bmatrix}. \tag{2}$$

Adding the translation to the affine transformation matrix,

$$\boldsymbol{A} = \begin{bmatrix} 1 & 0 & \\ 0 & 1 & \boldsymbol{T} \\ 0 & 0 & 1 \end{bmatrix} \cdot \boldsymbol{E}, \tag{3}$$

where $\boldsymbol{T}$ is the matrix containing translation transformation information,

$$\boldsymbol{T} = \begin{bmatrix} -x_{\Delta i} \\ -y_{\Delta i} \end{bmatrix}. \tag{4}$$

Adding the rotation angle to the affine transformation matrix with the rotation point (x_0, y_0),

$$\boldsymbol{B} = \begin{bmatrix} 1 & 0 & +x_0 \\ 0 & 1 & +y_0 \\ 0 & 0 & 1 \end{bmatrix} \cdot \begin{bmatrix} & \boldsymbol{R} & 0 \\ 0 & 0 & 1 \end{bmatrix} \cdot \begin{bmatrix} 1 & 0 & -x_0 \\ 0 & 1 & -y_0 \\ 0 & 0 & 1 \end{bmatrix} \cdot \boldsymbol{A}, \tag{5}$$

where $\boldsymbol{R}$ is the matrix containing rotational transformation information,

$$\boldsymbol{R} = \begin{bmatrix} \cos \alpha_{\Delta i} & -\sin \alpha_{\Delta i} \\ \sin \alpha_{\Delta i} & \cos \alpha_{\Delta i} \end{bmatrix}. \tag{6}$$

After the affine transformation of matrix $\boldsymbol{B}$, the next nine images are translated and rotated so that their regions to be detected are aligned with the first image. At this point, the first image is again subtracted and the vibration interference contours obtained by the fault detection algorithm are significantly reduced, as shown in Fig. 15.

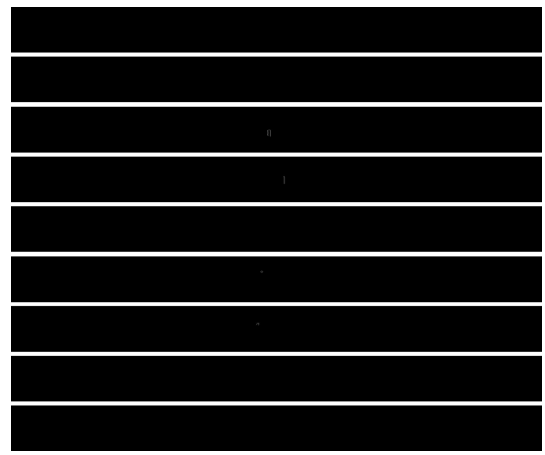

Fig. 15 Nine subtraction images after adding anti-vibration interference algorithm

It can be seen that after adding the anti-vibration interference algorithm, the oblique contours are successfully eliminated. The remaining contours that are significantly different from the fault contours can be filtered out by length and width thresholds. At this point, none of the fault detection algorithm's contour thresholds are satisfied, thus preventing false alarms. Comparing the nine subtraction images before and after adding the anti-vibration interference algorithm, the results are shown in Table 1.

Table 1 Number and area of interference contours before and after adding anti-vibration interference algorithm

Image	Total number of interference contours		Total area of interference contours	
	Before adding	After adding	Before adding	After adding
1	5	0	152	0
2	1	0	10	0
3	13	1	557	54
4	9	1	323	32
5	0	0	0	0
6	1	1	14	14
7	11	1	615	18
8	5	0	170	0
9	0	0	0	0
Total	45	4	1 841	118

After adding the anti-vibration interference algorithm, the interference information contained in the subtraction images is significantly reduced. The total number of interference contours is reduced to 8.9% of the original, and the total area of interference contours is reduced to 6.4% of the original. The accuracy of the image after offset correction fully meets the requirements and achieves the desired effect of the anti-vibration algorithm. After combining the fault detection algorithm, the purpose of anti-vibration interference is achieved, the false alarm is greatly reduced, and the accuracy of detection is greatly enhanced. In summary, the workflow of the anti-vibration interference algorithm is shown in Fig. 16.

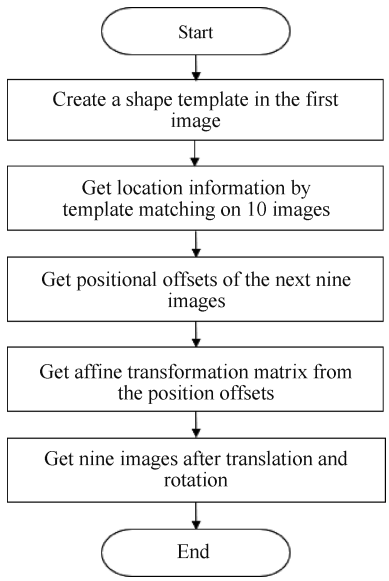

Fig. 16 Workflow of anti-vibration interference algorithm

3.4 Effect of yarn congestion fault detection algorithm

A total of 20 groups of video recordings of on-site yarn congestion faults were randomly selected, and the fault detection was carried out by the yarn congestion fault detection algorithm. The results are shown in Fig. 17. The detection time of the 20 groups of faults is not very different, with a detection time between 58 s and 63 s, and the average detection time is about 60 s. The successful detection rate of faults is 90%, and there are only two groups (7 and 19) of detection failures. Therefore, the detection time of the two groups (7 and 19) is not shown in Fig. 17. According to the results of the on-site investigation, the accuracy of this fault detection algorithm is also about 90%, which meets the production requirements.

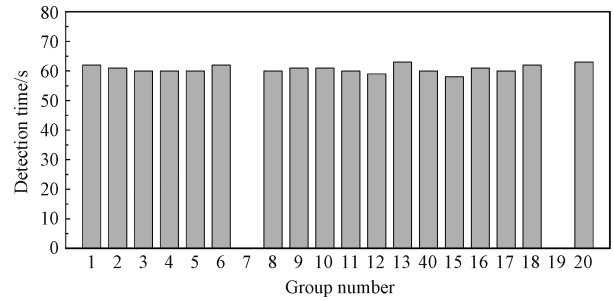

Fig. 17 Yarn congestion fault detection results

Analysis of the two detection failures revealed that they occurred because the yarn accumulation didn't meet the preset fault thresholds. The workers in the field had already identified and resolved the yarn congestion fault before the system alerts were triggered. The detection system's primary purpose is timely fault notification to prevent yarn waste and further yarn congestion fault

expansion. While manual detection typically requires over 60 s, cases where workers intervene before system alerts are still acceptable, as they achieve the same operational objective. In addition, the algorithm was used to detect 523 groups of yarn congestion faults collected in the field, and 477 groups were successfully detected with an accuracy rate of 91.2%, which met the production requirements. Overall, the fault detection algorithm for yarn congestion fault at the reed teeth position can detect the fault more accurately in a short time, offering a certain degree of real-time performance and accuracy.

4 Conclusions

This research combined the actual situation of the factory and adopted the machine vision technology to deal with the yarn congestion fault. The hardware equipment was set up in the factory, and the fault detection algorithm was designed by analyzing the characteristics of yarn congestion fault and vibration interference. It could detect the yarn congestion fault in a short time and remind workers to deal with it in time. The real-time performance and accuracy of the algorithm were verified in the field, which met the production requirements of industrial sites.

References

[1] XIAO H B. Technological development and outlook of sizing machine [J]. *China Textile Leader*, 2013(2): 54, 56-57. (in Chinese)

[2] YANG Z Q. Modernization of sizing engineering technology [J]. *Advanced Textile Technology*, 2002(3): 12-17. (in Chinese)

[3] ZHOU J, PAN R R, GAO W D. Application status and development trend of machine vision in textile[J]. *Cotton Textile Technology*, 2019, 47(2): 15-17. (in Chinese)

[4] ZENG K. Research on mobile robot obstacle avoidance based on optical flow method [D]. Tangshan: North China University of Science and Technology, 2017. (in Chinese)

[5] SCHNEIDER D, GLOY Y S, MERHOF D. Vision-based on-loom measurement of yarn densities in woven fabrics[J]. *IEEE Transactions on Instrumentation and Measurement*, 2015, 64(4): 1063-1074.

[6] SHI P F, BAI R L, YANG W H, et al. Broken yarn detection system on warping machine based on machine vision [J]. *Journal of Donghua University (Natural Science)*, 2011, 37(6): 750-754, 760. (in Chinese)

[7] ZHANG J L, LI Q. Online cheese package yarn density detection system based on machine vision [J]. *Journal of Textile Research*, 2020, 41(6): 141-146. (in Chinese)

[8] HALEEM N, BUSTREO M, DEL BUE A. A computer vision based online quality control system for textile yarns [J]. *Computers in Industry*, 2021, 133: 103550.

[9] XU C Q, WANG J L, TAO J, et al. A knowledge augmented deep learning method for vision-based yarn contour detection [J]. *Journal of Manufacturing Systems*, 2022, 63: 317-328.

[10] DLAMINI S, KAO C Y, SU S L, et al. Development of a real-time machine vision system for functional textile fabric defect detection using a deep YOLOv4 model [J]. *Textile Research Journal*, 2022, 92(5/6): 675-690.

[11] ZUO B, WANG F L. Surface cutting defect detection of magnet using Fourier image reconstruction [J]. *Computer Engineering and Applications*, 2016, 52(3): 256-260, 265. (in Chinese)

[12] KHANAL S R, SILVA J, GONZALEZ D G, et al. Fabric hairiness analysis for quality inspection of pile fabric products using computer vision technology [J]. *Procedia Computer Science*, 2022, 204: 591-598.

[13] GÜLTEKİN E, ÇELİK H İ, DÜLGER L C, et al. Image processing applications on yarn characteristics and fault inspection[J]. *Tekstil Ve Mühendis*, 2019, 26(116): 340-345.

[14] MUSA E. Line-laser-based yarn shadow sensing break sensor [J]. *Optics and Lasers in Engineering*, 2011, 49(3): 313-317.

[15] XIA X M, MENG S, PAN R R, et al. On-line detection of warp collision and reed embedding based on improved inter-frame difference method [J]. *Journal of Textile Research*, 2021, 42(6): 91-96. (in Chinese)

[16] LI C Z, WEI K H, ZHAO Y B, et al. Improvement of high-speed detection algorithm for nonwoven material defects based on machine vision [J]. *Journal of Donghua University (English Edition)*, 2024, 41(4): 416-427.

[17] GAO W D, JIANG W M, WANG J G, et al. Technological development history and prospect of domestic sizing machine [J]. *Cotton Textile Technology*, 2023, 51(10): 41-46. (in Chinese)

基于机器视觉的浆纱机拥纱故障检测

李经纬，邹　鲲*，赵　晨
东华大学 机械工程学院，上海 201620

摘　要：在浆纱过程中，浆纱机筘齿位置的纱线会出现拥纱故障，目前一般采用人工检查的方式处理拥纱故障。浆纱生产线范围大，全天运行，处理不及时会造成较大的纱线浪费。该研究开发了一种基于机器视觉的浆纱机筘齿拥纱故障检测算法。通过对拥纱故障和干扰轮廓特征的分析，确定了图片相减识别故障的基本思路。针对图片相减后出现的干扰信息，确定了 Canny 边缘提取和均值滤波的图像预处理方法。根据故障大小和位置特点设计了基于帧间差分的故障轮廓识别算法。针对摄像头振动干扰，研究了基于仿射变换的防振动干扰算法，确定了筘齿拥纱总的故障检测算法。对 20 组现场数据进行检测，检测率达到 90%。该故障检测算法实现了对浆纱机拥纱故障的自动检测，具有一定的实时性和准确性。

关键词：机器视觉；筘齿拥纱；故障检测；帧间差分；仿射变换